Int. J. Electrochem. Sci., 16**(2021)** Article Number: 21115, doi: 10.20964/2021.11.01

International Journal of ELECTROCHEMICAL SCIENCE
www.electrochemsci.org

Short Communication

Fabrication of N-doped TiO_2 Nanorods and Its Visible-Light Photocatalytic Activity for Resorcinol Degradation in Wastewater

Zaiyu Zhang[1,*], *Yuan Yang*[1], *Dongling Cheng*[2,*]

[1] Hunan Key Laboratory of Dong Medicine Research Institute, Hunan University of Medicine, Huaihua, 418000, China
[2] College of Water Resources and Architectural Engineering, Northwest A＆F University, Yangling, 712100, China
[*]E-mail: zaiyuzhang75@163.com, donglingcheng2020@126.com

Received: 1 July 2021/ *Accepted:* 18 August 2021 / *Published:* 10 October 2021

This work was focused on the synthesis of N-doped TiO_2 nanorods as photocatalyst and its visible-light photocatalytic activity to degrade resorcinol as phenolic pollutants in wastewater. Pure TiO_2 and N-doped TiO_2 NRs were synthesized using a solvothermal process. The analyses of morphology and structure of prepared photocatalysts by TEM and XRD showed that well-defined mesoporous nanorods in anatase phase were synthesized. The result of optical characterization showed that the band gap values of TiO_2 and N-doped TiO_2 NRs were obtained 3.04 and 2.31 eV, respectively, indicating the band gap of N-doped TiO_2 NRs was greatly narrower than the pure TiO_2 NRs. The results of EIS analysis showed lower resistance of carrier transfer for the doped sample. The Results of the photocatalytic study showed that the complete treatments of 100 mg/l resorcinol were obtained at 120 and 95 minutes under UV irradiation for pure TiO_2 and N-doped TiO_2 NRs, respectively, and complete removal was obtained at 130 and 85 minutes under visible light irradiation for pure TiO_2 and N-doped TiO_2 NRs, respectively. Therefore, the higher degradation rate of resorcinol on N-doped TiO_2 NRs under visible light irradiation was observed which can be attributed to the narrowing band gap of doped sample and formation of an impurity energy level, avoiding the recombination between e^- and h^+.

Keywords: Degradation of phenolic pollutants**;** Wastewater; Photocatalyst; N-doped TiO_2 nanorods

1. INTRODUCTION

Resorcinol (m-dihydroxybenzene, $C_6H_4(OH)_2$ as a 1,3-isomer of benzenediol is a toxic phenolic compound that its chemistry provide valuable characteristic and products for development in textile, paper, rubber, paints, plastics, steel, pharmaceuticals, petroleum refinery, petrochemical, wood, chemical fertilizers, cosmetic and dye industries [1-3]. It is most widely used as an antiseptic and

disinfectant in the treatment of psoriasis, eczema, acne, seborrheic dermatitis, corns, calluses, warts, and other skin disorders. It is used in the synthesis of resins, glue, pesticide and many organic chemical compounds [4-6].

Studies showed that this organic compound has polluted industrial and medical wastewaters due to its numerous applications [7-9]. Resorcinol is hazardous pollutants because of its potential harmfulness to human health, and damages aquatic organisms and crops [10, 11]. For example, Resorcinol can disrupt the function of the central nervous system and endocrine system and lead to respiratory problems and thyroid disruptors [12-14]. Moreover, it causes skin and eye irritants and skin sensitizers [15-17].

Therefore, it is necessary to remove this toxic phenolic compound from wastewaters before discharge [18-20]. The methods such as activated carbon adsorption, distillation, solid-phase extraction, biodegradation, emulsion liquid membrane, electrocoagulation, chemical oxidation, electro-oxidation, peroxidase treatment, activated sludge process and photodegradation are the common methods for the removal of resorcinol [21-23]. Among them, the photodegradation process based on photocatalysis has attracted intense attention due to low cost, environmentally friendly and high degradation rate [24-27]. Furthermore, photocatalysts based on nano-modified materials exhibits high surface-to-volume ratio properties and promote photodegradation efficiency [28-30]. Although much research has been done on the photodegradation of toxic phenolic compounds from wastewaters, no reports are available on the photodegradation behavior of N-doped TiO_2 nanorods for resorcinol degradation in wastewater. Therefore, this work focused on synthesizing N-doped TiO_2 nanorods as photocatalysts and their visible-light photocatalytic activity to degrade resorcinol as phenolic pollutants in wastewater.

2. EXPERIMENT

2.1. Synthesis

The solvothermal process was applied to the synthesis of N-doped TiO_2 NRs as following steps [31]: the mixture of 13 g titanium sulfate (94%, Beijing Wan Yun Hua Rui Chemical Co., Ltd., China), 5 g urea (98%, Sigma Aldrich)and 20 mL of dichloromethane (99.8%, Sigma Aldrich) were prepared and transferred to a 50 ml autoclave at 175°C for 12 hours. After cooling, the resulted product was filtered, rinsed with deionized water, and dried at 90 °C for 4 hours. in order to doping the produced TiO_2, 3g as-synthesized TiO_2 powder was added to a mixture of 20 mL of 7MNaOH (98%, Sigma Aldrich), 11 mL deionized water and 14 mL ethanol (99.9%, Shandong Aojin Chemical Technology Co., Ltd., China). The mixture was transferred into a 50 ml autoclave at 120 °C for 18 hours. After cooling, the synthesized N-doped TiO_2 was filtered, rinsed with deionized water, and dried at 90 °C for 4 hours.

2.2. Photocatalytic study

For the study of photocatalytic activity, 50 mg of N-doped TiO_2 was added to 45 mL of resorcinol (99.0%, Sigma Aldrich) in a Pyrex glass vessel under continuous magnetic stirring. Before the photocatalytic experiments, the solution was stirred for 30 minutes in darkness to reach the equilibrium adsorption/desorption equilibrium of resorcinol molecules on the catalyst. The reaction was conducted on the Pyrex glass vessel under irradiation of UV lamp mercury 300 W and Xenon arc lamp (420 nm < λ < 800 nm, Abet, Japan) as visible light and UV sources, respectively. The mixture of resorcinol and N-doped TiO_2 was filtered using a syringe filtration system (pore size 0.2 and 0.45 μm, Sigma-Aldrich). Subsequently, 2 mL of the filtrated solution was monitored using UV–vis spectrophotometer (Shimadzu, UV/vis spectrophotometer UV-1280, Japan).

2.3. Characterization

The structural characterization of samples was carried out with an X-ray diffractometer (XRD, Philips, X'Pert PRO MPD, and Holland). The transmission electron microscopy (TEM-2100F, JEOL Ltd., Tokyo, Japan) was used to study the morphology of the synthesized photocatalysts. The optical properties of prepared samples were analyzed using UV–visible spectra on UV–visible spectrophotometer (UV–visible DRS, TU1901, and Beijing, China). Electrochemical impedance spectroscopy (EIS) analysis was performed on an electrochemical workstation (CHI760E, Shanghai Chenhua CO., China) using three-electrode cells which contained the TiO_2 or N-doped TiO2 as working electrode, a saturated calomel electrode (SCE) as the reference electrode and Pt foil as the counter electrode. EIS experiments were carried out in electrolyte solution of 0.5 M Na_2SO_4 pH 7 in the frequency range from 1 to 10^6Hz at 5 mV an AC perturbation signal under open circuit potential condition.

3. RESULT AND DISCUSSION

3.1. Structural and optical characterizations

TEM images of the TiO_2 and N-doped TiO_2 is shown in Figure 1. As observed from Figure 1a, the TiO_2 is made up from well-defined nanorod structures, having an average length around 500nm and a diameter around 50nm. It can be observed from Figure 1b, the N-doped TiO_2 nanorods are synthesized in the mesoporous structure due to the introduction of N in TiO_2 in the hydrothermal process [32]. The mesoporous structure of nanorods shows remarkable enhancement in specific surface area, which is larger than that of a smooth surface of undoped TiO_2. This mesoporous structure can facilitate the charge transfer and improve photo-electrochemistry activity because the 1D nanostructure and higher specific surface area of N-doped TiO_2 [33-35].

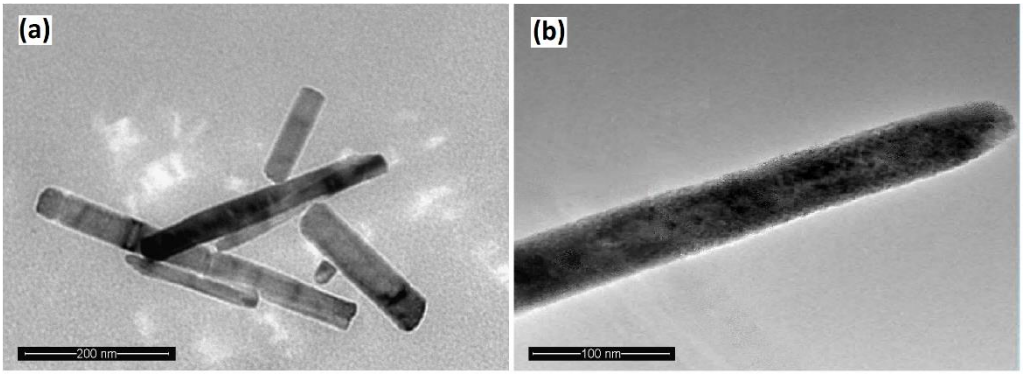

Figure 1. TEM images of (a) TiO_2, and (b) N-doped TiO_2 NRs.

Figure 2 shows the result of XRD characterization of TiO_2 and N-doped TiO_2. As shown in Figure 2a, XRD pattern of TiO_2 shows the diffraction peaks at 2θ = 25.38°, 38.18°, 48.08°, 53.72°, 55.02°, 62.79°, 69.20°, 70.72° and 75.06° which are indexed to the (101), (004), (200), (105), (211), (204), (116), (220) and (215) planes of the anatase phase [36], respectively (JCPDS card no. 21-1272). Studies have been suggested the anatase crystal structure can show better photocatalysis because of a larger surface area than rutile or brookite phase of TiO_2 [37, 38].

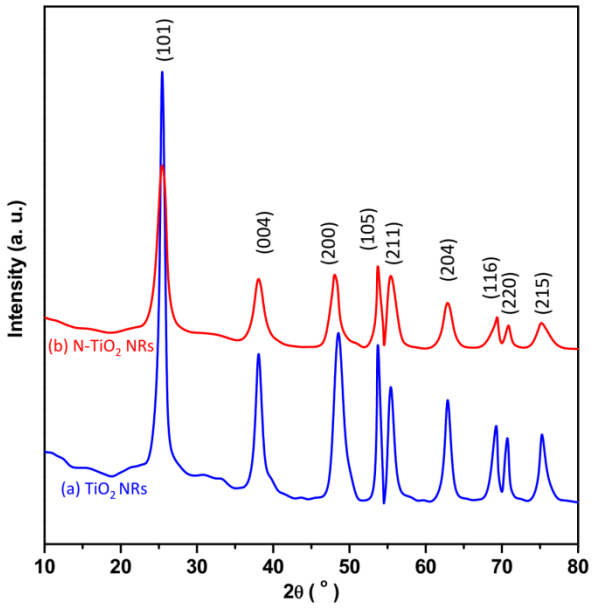

Figure 2. XRD characterization of (a) TiO_2 and (b) N-doped TiO_2

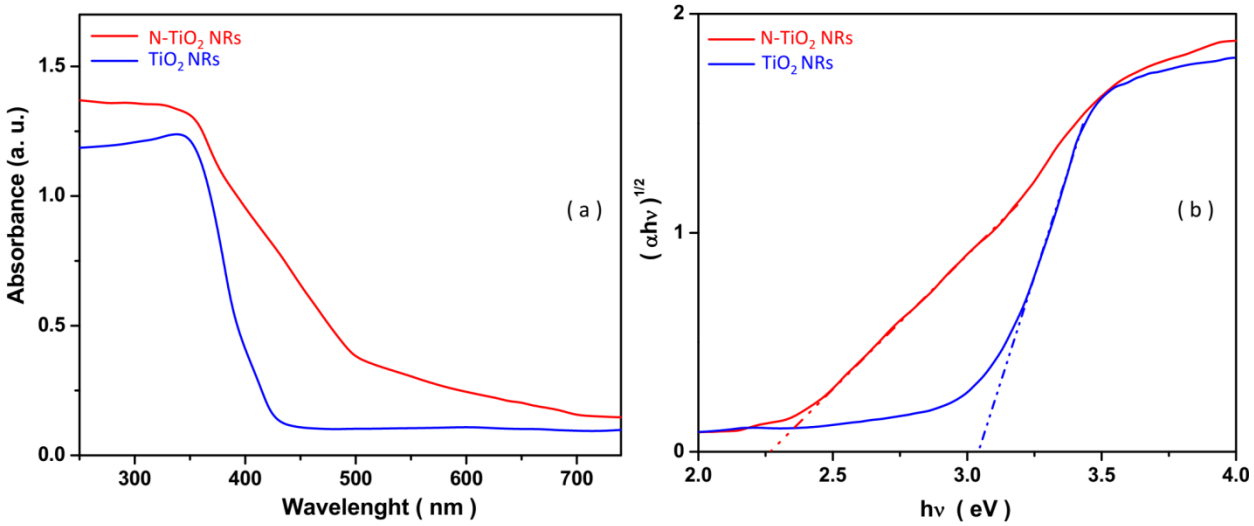

Figure 3. (a) UV-Visible absorption spectra and (b) Taucs plot of TiO_2 and N-doped TiO_2 NRs.

Furthermore, the anatase phase exhibits higher stability at relatively lower temperatures than rutile and brookite phases [38]. It can be observed from Figure 2b that there is the same diffraction peaks with lower intensity for the N-doped TiO_2 which recommends to the nitrogen doping change surface and crystallinity of TiO_2, and indicating a loss of crystallinity due to lattice distortion [39]. Nonetheless, the anatase phase of N-doped TiO2 reveals the presence of nitrogen not creates a new crystal phase and dopant only influence the crystal lattice. In addition, doping cause to shift the diffraction peaks of anatase TiO_2 to the higher angles because of defects or incorporation of a larger amount of doped ions into the TiO_2 structure [40], which in agreement with the TEM results for the generation of the mesoporous structure of N-doped TiO_2.

The result of optical characterization of TiO_2 and N-doped TiO_2 NRs are shown in Figure 3. Obviously, it can be found from Figure 3a, the feature of UV–vis absorbance spectra of TiO_2 is similar to that N-TiO_2. The absorption edge of doped nanorods is red-shifted which typically exhibits a considerable absorption in the visible region that is a characteristic feature of absorption spectra of nitrogen-doped TiO_2 [41-43]. Viswanathan and Krishnamurthy [44] suggested the formation of new adsorption centers could be one of the reasons for the shift of the absorption edge to the visible range. Figure 3b shows the result of the calculation of band gap energy using Tauc's equation (1) [45]:

$$(\alpha h\nu)^{\frac{1}{2}} = B(h\nu - E_g) \qquad (1)$$

Where α is the absorption coefficient, Eg (eV) is the band gap energy, h the Planck's constant ($4.135667696\times10^{-15}$eV.s), and B is the absorption constant. The Eg values are determined by extrapolating the linear fit of the Tauc plot onto the energy axis. The Eg of TiO_2 and N-doped TiO2 NRs are obtained 3.04 and 2.31 eV, respectively, indicating the Eg of N-doped TiO_2 NRs are greatly narrower than pure TiO_2 NRs, and improving the photocatalytic performance in visible light [46]. Wellia et al. [47] and Cheng et al. [48] also reported the decrease of band gap from 3.09 eV to be 2.89

eV and from 3.10 eV to be 2.85 eV, respectively due to nitrogen doping. This change is associated with the introduction of nitrogen in the crystal structure phase of TiO_2. Studies have been shown in the doping process, the substitution of nitrogen with oxygen in TiO_2 leads to narrow the band gap due to the nitrogen 2p states mixed with oxygen 2p states and located just above the top of the oxygen 2p valence band that it exhibits a significant red-shift of the absorption edge into the visible region [46]. Thus, it demonstrates that nitrogen is the best and low-cost nonmetal dopant.

3.2. Electrochemical study

The EIS analysis was applied to study the charge-carrier migration of the TiO_2 and N-doped TiO_2 NRs. Figure 4 shows the Nyquist plots which contain one semicircle. The diameter of the semicircle has been interpreted as charge transfer resistance that controls the kinetics at the electrode/electrolyte interface [49].As observed, the small diameter is obtained for N-doped TiO_2 NRs, indicating to lower resistance of carrier transfer, and thereby there are the faster and higher electron mobility on the N-doped TiO_2 NRs surface that it means the doped structure can enhance the separation of the photo-generated electron-hole pairs [50].

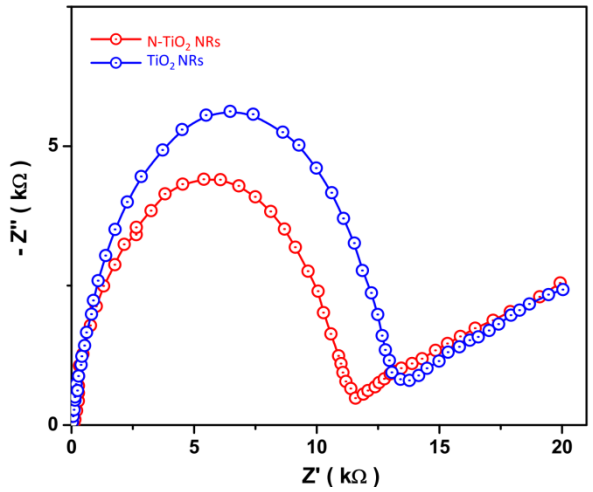

Figure 4. Nyquist plots of TiO_2 and N-doped TiO_2 NRs in electrolyte solution of 0.5 M Na_2SO_4 pH 7 in the frequency range from 1 to 10^6 Hz at 5 mV an AC perturbation signal under open circuit potential condition.

3.3. Photocatalytic study

Figure 5 shows the removal efficiency of 100 mg/l resorcinol in 1 g/L of pure TiO_2 and N-doped TiO_2 NRs in dark and under UV and visible light irradiations. It can be observed from Figure 5a, there is less than 0.8 % removal efficiency is obtained for resorcinol in the first 40 minutes in darkness that this poor removal efficiency implied the important role of light illumination in degradation reactions. The complete treatments of resorcinol are obtained at 120 and 95 minutes under UV irradiation for pure TiO_2 and N-doped TiO2 NRs, respectively. Figure 5b shows that there is the complete removal of 100 mg/l resorcinol at 130 and 85 minutes under visible light irradiation for pure

TiO_2 and N-doped TiO2 NRs, respectively. The higher degradation rate of the undoped sample under UV irradiation than that under visible irradiation shows the great influence to photodegradation under UV because of its band gap value and largely photocatalytic activity in the UV region [51]. The higher degradation rate under visible light irradiation is belonging to N-doped TiO_2 NRs due to the narrowing of the band gap of the doped sample, formation of an impurity energy level, and oxygen vacancies which allows avoiding the recombination between e^- and h^+[46, 52]. It can facilitate the visible light activity because of the creation of intra bands as a result of the mixing of nitrogen 2p states with oxygen 2p [44], which is in agreement with the optical results. Moreover, according to SEM and TEM results, the mesoporous structure of N-doped TiO2 NRs with high surface area, as well as the large amount of oxygen vacancies, promoted the light-harvesting capacity, photoinduced charge carriers separation capability, reactant molecule adsorption, and activation characteristics [53].

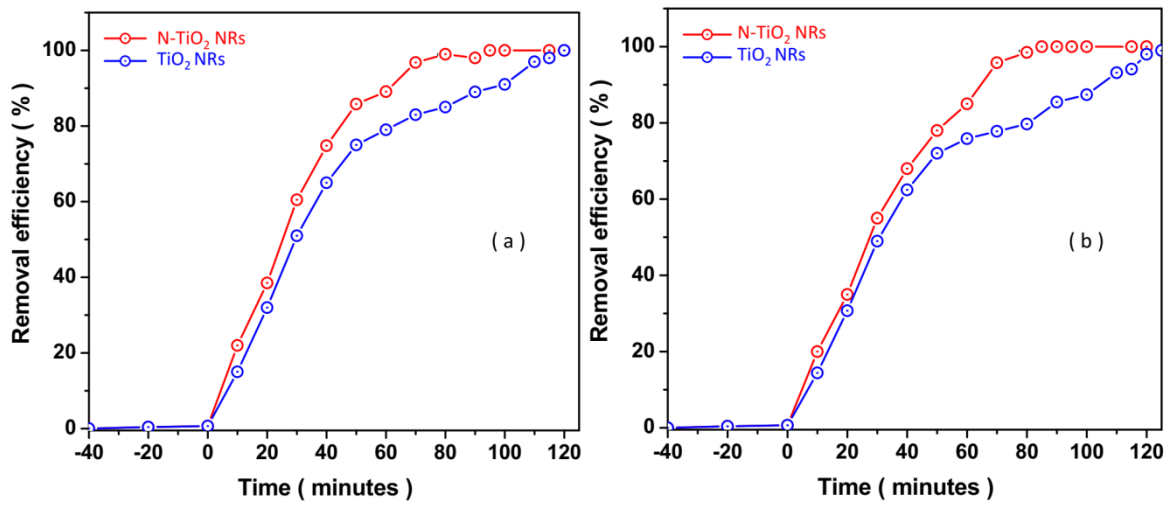

Figure 5. Removal efficiency of 100 mg/l resorcinol in 1 g/L of pure TiO_2 and N-doped TiO2 NRs under (a) UV and (b) visible light irradiations

The effect of the concentration of photocatalyst on the removal efficiency of 100 mg/l resorcinol was investigated. Figure 6 shows the degradation efficiencies of resorcinol in 0 (blank), 0.1, 0.5, 1 and 2 g/L of N-doped TiO2 NRs visible light irradiation. As seen, the removal efficiency of blank is obtained 5.4% after 170 minutes visible light irradiation, which refers to the great effect of photocatalyst on removal of resorcinol underexpose the visible light. The 100% removal of resorcinol is obtained at 170, 115, 85 and 90 minutes visible light irradiation for 0.1, 0.5, 1 and 2 g/L of N-doped TiO2 NRs.

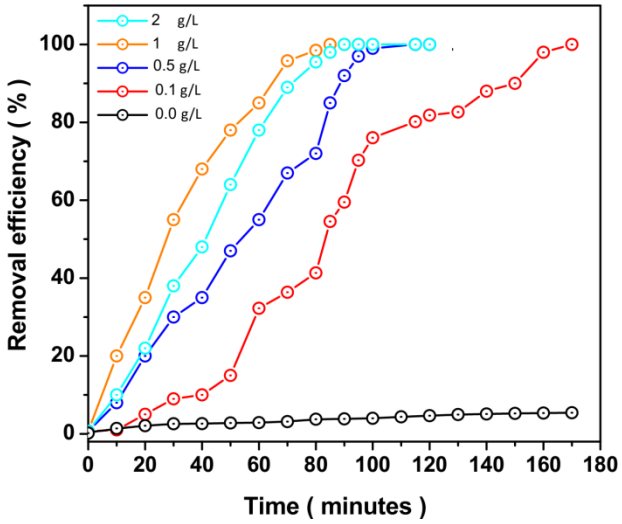

Figure 6. Degradation efficiencies of 100 mg/l resorcinol in 0 (blank), 0.1, 0.5, 1, 5 g/L of N-doped TiO_2 NRs visible light irradiation

Table 1. Comparison between the obtained results of this study with other reported photocatalyst for degradation of resorcinol.

Photocatalyst	Resorcinol content (mg/l)	Concentration of photocatalyst (g/L)	Light source	Degradation time (minute)	Degradation efficiency (%)	Ref.
TiO_2 NRs	100	1	UV visible	120 130	100 100	This work
N-doped TiO_2 NRs	100	1	UV visible	95 85	100 100	This work
TiO_2 nanoparticles/ mesoporous carbon	100	0.15	UV	150	78	[58]
Fe^{+3}/TiO_2	20	0.1	UV	237	100	[59]
Cu^{+2}/TiO_2	30	0.02	UV	250	100	[60]
$Bi_4O_5Br_2$	18	1.5	visible	180	93.8	[61]
TiO_2	30	1	visible	120	93	[62]
TiO_2nanowires	20	1	UV	180	98	[63]
TiO_2 nanoparticles	20	1	UV	180	98	[63]
TiO_2-P25	20	1	UV	180	83	[63]
ZnO	20	1	UV	360	77	[64]
Ag_2O/ZnO nanoparticles	20	1	UV	360	92	[64]
Ag_2O/ZnOheterostructure	20	1	UV	297	100	[64]

Accordingly, the addition of photocatalyst content to1 g/Lin the reactor increases the degradation rate and significant removal efficiency is obtained for higher concentration of N-doped TiO2 NRs. It is suggested increasing the concentration of photocatalyst lead to increasing mass and surface area of photoctalyst in the reactor, and enhance the effective illumination of the catalyst surface by the visible light, and produced hydroxyl radical ($^{\bullet}OH$) [54-56]. For concentration of photocatalyst more than 1 g/L, the high density of particles cause the shielding effect and scattering of the visible

light [54], hence the reactor volume is only partially illuminated and the removal efficiency is lower than the case with 1 g/L concentration of photocatalyst.

Table 1 presents the comparison between the obtained results of this study with other reported photocatalyst for degradation of resorcinol. It can be found that the considerable degradation rate of resorcinol is achieved on N-doped TiO2 NRs photocatalyst which represented the enhancement of surface area-to-volume ratio and absorption capability of mesoporous nanorods. Moreover, it is reported that the doping process can form new energy levels of impurity top of the valence band of TiO_2 which can act as an electron sink to reduce the recombination rate [57].

In order to study the applicability of degradation performance of the proposed photocatalyst in a real sample of wastewater, the photocatalytic degradation reactions of 7 mg/l resorcinol prepared from deionized water as a model solution (Figure 7a) and a real sample of industrial wastewater (Figure 7b) was investigated. It can be observed from UV–Vis spectra in Figure 7 that the intensity of the absorption peaks continuously decreases during the photodegradation for both samples and disappeared after 12 and 16 minutes degradation in model solution and a real sample, respectively, indicating the degradation time for a prepared solution with a real sample of industrial wastewater is higher that the model solution due to the presence wide range of pollutants from wastewater. Thus, the novelty of this work is the facile and scalable synthesis N-doped TiO_2 NRs as low-cost photocatalyst for fast resorcinol treatment in wastewater.

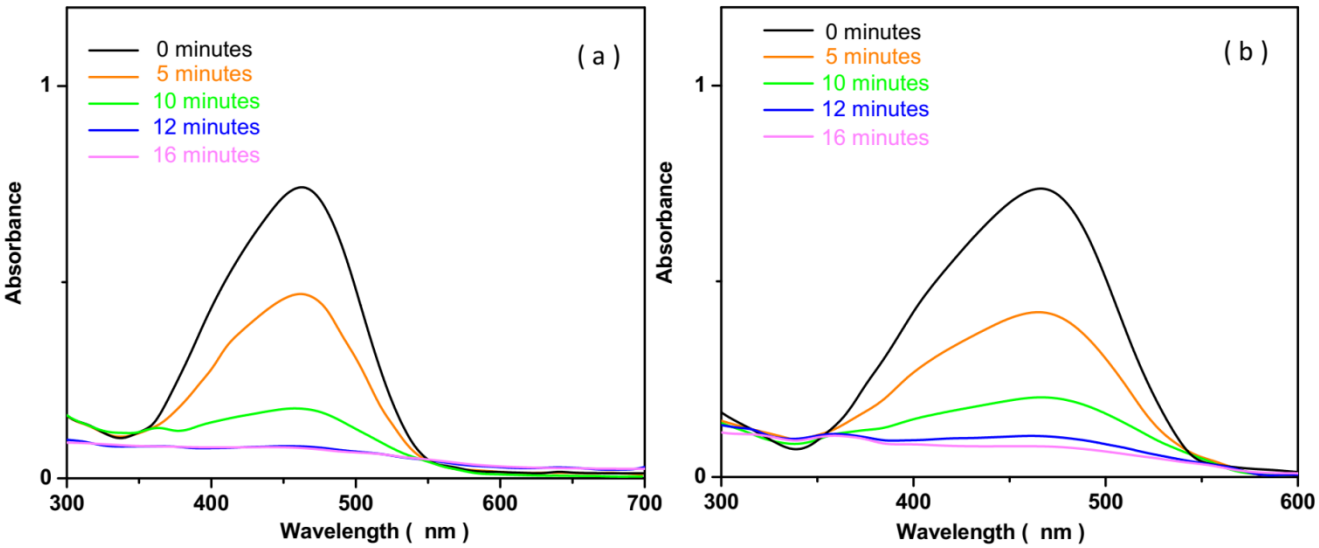

Figure 7. UV–Vis spectra of photocatalytic degradation reaction of 7 mg/l resorcinol prepared from (a) deionized water as model solution and (b) real sample with respect to different irradiation times by1 g/L of N-doped TiO_2 NRs photocatalyst.

4. CONCLUSION

This work presented the fabrication of pure and N-doped TiO2 nanorods as photocatalysts to degrade resorcinol as phenolic pollutants in wastewater. The solvothermal process was applied to the

synthesis of TiO_2 and N-doped TiO_2 NRs. Results of the morphology and structure analyses showed that well-defined mesoporous nanorods in the anatase phase were synthesized. The result of optical studies showed that the band gap values of pure and the doped samples were obtained 3.04 and 2.31 eV, respectively, indicating the band gap of the doped sample was narrower than that of the pure sample. The results of electrochemical study exhibited the lower resistance of carrier transfer for the doped sample. The Results of the photocatalytic study showed that the complete treatments of 100 mg/l resorcinol were obtained at 120 and 95 minutes under UV irradiation for pure TiO_2 and N-doped TiO_2 NRs, respectively, and complete removal were obtained at 130 and 85 minutes under visible light irradiation for pure TiO_2 and N-doped TiO2 NRs, respectively. Therefore, the higher visible-light photocatalytic activity of doped TiO_2 NRs is obtained to degrade resorcinol because of the narrowing of the band gap of the doped sample, formation of an impurity energy levels, and oxygen vacancies which allows avoiding the recombination photogenerated charges.

References

1. R. Aghav, S. Kumar and S. Mukherjee, *Journal of hazardous materials*, 188 (2011) 67.
2. W.-Y. Huang, G.-Q. Wang, W.-H. Li, T.-T. Li, G.-J. Ji, S.-C. Ren, M. Jiang, L. Yan, H.-T. Tang and Y.-M. Pan, *Chem*, 6 (2020) 2300.
3. Y. Orooji, B. Tanhaei, A. Ayati, S.H. Tabrizi, M. Alizadeh, F.F. Bamoharram, F. Karimi, S. Salmanpour, J. Rouhi and S. Afshar, *Chemosphere*, 281 (2021) 130795.
4. C. Raril and J.G. Manjunatha, *Analytical and Bioanalytical Electrochemistry*, 10 (2018) 488.
5. Y. Duan, Y. Liu, Z. Chen, D. Liu, E. Yu, X. Zhang, H. Fu, J. Fu, J. Zhang and H. Du, *Green Chemistry*, 22 (2020) 44.
6. N. Naderi, M. Hashim, J. Rouhi and H. Mahmodi, *Materials science in semiconductor processing*, 16 (2013) 542.
7. S. Suresh, V.C. Srivastava and I.M. Mishra, *International Journal of Energy and Environmental Engineering*, 3 (2012) 1.
8. H. Liu, X.-X. Li, X.-Y. Liu, Z.-H. Ma, Z.-Y. Yin, W.-W. Yang and Y.-S. Yu, *Rare Metals*, 40 (2021) 808.
9. H. Karimi-Maleh, Y. Orooji, F. Karimi, M. Alizadeh, M. Baghayeri, J. Rouhi, S. Tajik, H. Beitollahi, S. Agarwal and V.K. Gupta, *Biosensors and Bioelectronics*, 184 (2021) 113252.
10. S. Zhang, S. Zhao, S. Huang, B. Hu, M. Wang, Z. Zhang, L. He and M. Du, *Chemical Engineering Journal*, 420 (2021) 130516.
11. L. Zhang, J. Zheng, S. Tian, H. Zhang, X. Guan, S. Zhu, X. Zhang, Y. Bai, P. Xu and J. Zhang, *Journal of Environmental Sciences*, 91 (2020) 212.
12. Y. Yang, H. Chen, X. Zou, X.-L. Shi, W.-D. Liu, L. Feng, G. Suo, X. Hou, X. Ye and L. Zhang, *ACS applied materials & interfaces*, 12 (2020) 24845.
13. X. Wang, Z. Feng, B. Xiao, J. Zhao, H. Ma, Y. Tian, H. Pang and L. Tan, *Green Chemistry*, 22 (2020) 6157.
14. Q. Hu, W. Zhang, Q. Yin, Y. Wang and H. Wang, *Spectrochimica Acta Part A: Molecular and Biomolecular Spectroscopy*, 244 (2021) 118864.
15. B.S. Lynch, E.S. Delzell and D.H. Bechtel, *Regulatory toxicology and pharmacology*, 36 (2002) 198.
16. Z. Lei, S. Hao, J. Yang, L. Zhang, B. Fang, K. Wei, Q. Lingbo, S. Jin and C. Wei, *Chemosphere*, 270 (2021) 128646.

17. X.-Q. Lin, Z.-L. Li, B. Liang, H.-L. Zhai, W.-W. Cai, J. Nan and A.-J. Wang, *Water research*, 162 (2019) 236.
18. Z. Ni, X. Cao, X. Wang, S. Zhou, C. Zhang, B. Xu and Y. Ni, *Coatings*, 11 (2021) 749.
19. X. Zhu, F. Lin, Z. Zhang, X. Chen, H. Huang, D. Wang, J. Tang, X. Fang, D. Fang and J.C. Ho, *Nano letters*, 20 (2020) 2654.
20. Z. Li, Y. Shi, A. Zhu, Y. Zhao, H. Wang, B.P. Binks and J. Wang, *Angewandte Chemie International Edition*, 60 (2021) 3928.
21. L. Zhang, M. Zhang, S. You, D. Ma, J. Zhao and Z. Chen, *Science of The Total Environment*, 780 (2021) 146505.
22. Z. Lei, S. Hao, J. Yang and X. Dan, *International Journal of Hydrogen Energy*, 45 (2020) 19280.
23. J. Rouhi, S. Mahmud, S.D. Hutagalung and N. Naderi, *Electronics letters*, 48 (2012) 712.
24. D. Yuan, M. Sun, M. Zhao, S. Tang, J. Qi, X. Zhang, K. Wang and B. Li, *International Journal of Electrochemical Science*, 15 (2020) 8761.
25. Y. Shen, F. Li, S. Li, D. Liu, L. Fan and Y. Zhang, *International Journal of Electrochemical Science*, 7 (2012) 8702.
26. Q. Li, K. Wang, X. Lu, R. Luo, M. Zhang, C. Cui and G. Zhu, *International Journal of Electrochemical Science*, 15 (2020) 9256.
27. A. Xu, B. Li, B. Zhan, S. Xue, R. Guo and W. Zhong, *International Journal of Electrochemical Science*, 12 (2017) 448.
28. B.O. Bica and J.V.S. de Melo, *Construction and Building Materials*, 252 (2020) 119120.
29. R. Savari, S. Soltanian, A. Noorbakhsh, A. Salimi, M. Najafi and P. Servati, *Sensors and Actuators B: Chemical*, 176 (2013) 335.
30. H. Karimi-Maleh, M.L. Yola, N. Atar, Y. Orooji, F. Karimi, P.S. Kumar, J. Rouhi and M. Baghayeri, *Journal of colloid and interface science*, 592 (2021) 174.
31. Z. He and H. He, *Applied surface science*, 258 (2011) 972.
32. S.A. Bakar and C. Ribeiro, *Journal of Photochemistry and Photobiology C: Photochemistry Reviews*, 27 (2016) 1.
33. A. Machín, K. Fontánez, J.C. Arango, D. Ortiz, J. De León, S. Pinilla, V. Nicolosi, F.I. Petrescu, C. Morant and F. Márquez, *Materials*, 14 (2021) 2609.
34. H. Savaloni, E. Khani, R. Savari, F. Chahshouri and F. Placido, *Applied Physics A*, 127 (2021) 1.
35. R. Savari, H. Savaloni, S. Abbasi and F. Placido, *Sensors and Actuators B: Chemical*, 266 (2018) 620.
36. S. Dai, Y. Wu, T. Sakai, Z. Du, H. Sakai and M. Abe, *Nanoscale research letters*, 5 (2010) 1829.
37. S. Safni, M.R. Wahyuni, K. Khoiriah and Y. Yusuf, *Molekul*, 14 (2019) 6.
38. J. Zhang, P. Zhou, J. Liu and J. Yu, *Physical Chemistry Chemical Physics*, 16 (2014) 20382.
39. M. Pal, U. Pal, J.M.G.Y. Jiménez and F. Pérez-Rodríguez, *Nanoscale research letters*, 7 (2012) 1.
40. L. Ntozakhe, R. Taziwa and H. Mungondori, *Materials Research Express*, 6 (2019) 0850a9.
41. S. Larumbe, M. Monge and C. Gomez-Polo, *IEEE Transactions on Magnetics*, 50 (2014) 1.
42. A. Khalilzadeh and S. Fatemi, *Clean Technologies and Environmental Policy*, 16 (2014) 629.
43. R. Hassanzadeh, A. Siabi-Garjan, H. Savaloni and R. Savari, *Materials Research Express*, 6 (2019) 106429.
44. B. Viswanathan and K. Krishanmurthy, *International journal of photoenergy*, 2012 (2012) 1.
45. H. Lin, C. Huang, W. Li, C. Ni, S.I. Shah and Y.-H. Tseng, *Applied Catalysis B: Environmental*, 68 (2006) 1.
46. J. Gomes, J. Lincho, E. Domingues, R.M. Quinta-Ferreira and R.C. Martins, *Water*, 11 (2019) 373.

47. D.V. Wellia, D. Fitria and S. Safni, *The Journal of Pure and Applied Chemistry Research*, 7 (2018) 25.
48. X. Cheng, X. Yu, Z. Xing and L. Yang, *Arabian Journal of Chemistry*, 9 (2016) S1706.
49. B.-A. Mei, J. Lau, T. Lin, S.H. Tolbert, B.S. Dunn and L. Pilon, *The Journal of Physical Chemistry C*, 122 (2018) 24499.
50. W. Wang, T. Ai and Q. Yu, *Scientific reports*, 7 (2017) 1.
51. S.A. Bakar and C. Ribeiro, *RSC advances*, 6 (2016) 36516.
52. A. Zaleska, *Recent patents on engineering*, 2 (2008) 157.
53. S. Sun, X. Yu, Q. Yang, Z. Yang and S. Liang, *Nanoscale Advances*, 1 (2019) 34.
54. W. Van de Moortel, M. Kamali, K. Sniegowski, L. Braeken, J. Degrève, J. Luyten and R. Dewil, *Water*, 12 (2020) 1672.
55. Y.-C. Tang, X.-H. Huang, H.-Q. Yu and L.-H. Tang, *International Journal of Photoenergy*, 2012 (2012) 1.
56. F. Chahshouri, H. Savaloni, E. Khani and R. Savari, *Journal of Micromechanics and Microengineering*, 30 (2020) 075001.
57. A.T. Kuvarega, R.W. Krause and B.B. Mamba, *Journal of Nanomaterials*, 2014 (2014) 1.
58. A. Rahmani, H. Rahimzadeh and S. Beirami, *DESALINATION AND WATER TREATMENT*, 144 (2019) 224.
59. S.W. Lam, K. Chiang, T.M. Lim, R. Amal and G.K.-C. Low, *Journal of Catalysis*, 234 (2005) 292.
60. S. Lam, K. Chiang, T. Lim, R. Amal and G.-C. Low, *Applied Catalysis B: Environmental*, 55 (2005) 123.
61. M. Li, Y. Cui, Y. Jin and H. Li, *RSC Advances*, 6 (2016) 47545.
62. J. Arana, C. Fernández Rodríguez, J. Herrera Melián, O. González Díaz and J. Pérez Peña, *Journal of solar energy engineering*, 130 (2008) 041002.
63. L. Al-Hajji, A.A. Ismail, M. Alsaidi, S. Ahmed, F. Almutawa and A. Bumajdad, *Journal of Nanoparticle Research*, 22 (2020) 1.
64. S.-M. Lam, J.-C. Sin, A. Abdullah and A. Mohamed, *Chemical Papers*, 67 (2013) 1277.